CYCLICALITY OF REAL WAGES IN THE USA AND GERMANY: NEW INSIGHTS FROM WAVELET ANALYSIS

Martyna Marczak*
Víctor Gómez**

D-2012-05

June, 2012

_____

* University of Hohenheim, Department of Economics, Schloss, Museumsfluegel, D-70593 Stuttgart, Germany, e-mail: marczak@uni-hohenheim.de
** Ministry of Finance and Public Administrations, Madrid, Spain, e-mail: vgomez@sepg.minhap.es.

This document is available at: http://www.sepg.pap.minhap.gob.es/SITIOS/SGPG/es-ES/PRESUPUESTOS/DOCUMENTACION/Paginas/Documentación.aspx

Abstract

This article provides new insights into the cyclical behavior of consumer and producer real wages in the USA and Germany. We apply two methods for the estimation of the cyclical components from the data: the approach based on the structural time series models and the ARIMA–model–based approach combined with the canonical decomposition and a band–pass filter. We examine the extracted cycles drawing on two wavelet concepts: wavelet coherence and wavelet phase angle. In contrast to the analysis in the time or frequency domains, wavelet analysis allows for the identification of possible changes in cyclical patterns over time. From the findings of our study, we can infer that the USA and Germany differ with respect to the lead–lag relationship of real wages and the business cycle. In the USA, both real wages are leading the business cycle in the entire time interval. The German consumer real wage is, on the other hand, lagging the business cycle. For the German producer real wage, the lead–lag pattern changes over time. We also find that real wages in the USA as well in Germany are procyclical or acyclical until 1980 and countercyclical thereafter.

JEL Classification: E32, C22, C32, J30

Keywords: Real wages, business cycle, wavelet analysis, wavelet phase angle, trend–cycle decomposition, structural time series model, ARIMA–model–based approach, band–pass filter

1 Introduction

The question of real wage behavior in the course of the business cycle has been analyzed in many studies, particularly in the US case. Most of the studies based on aggregate data concentrate on the analysis in the time domain, see for example, the detailed surveys of Abraham and Haltiwanger (1995) and Brandolini (1995) for the USA and the studies of Brandner and Neusser (1992) and Pérez (2001) for Germany. A disadvantage of common time–domain comovement tools as, for example, sample cross–correlations or regression coefficients of some cycle reference measure is that they are incapable of identifying detailed patterns of cyclicality since they do not differentiate between horizons at which comovement could be detected.

To overcome this shortcoming of the time domain analysis, some studies consider the comovements in the frequency domain where one is able to assess the relative importance of components with different periodicities for the observed behavior. The frequency–domain approach in the investigation of real wage cyclicality is followed in the works of, e.g., Marczak and Beissinger (2012), Hart et al. (2009) and Messina et al. (2009). Standard multivariate spectral techniques, such as cross–spectrum, coherency or phase angle, are, however, time–invariant. In order to additionally take time information into account, we propose to use wavelet analysis as an alternative tool to measure comovements between time series. Applications based on wavelet measures are already widespread in such disciplines as physics, meteorology, geology, medicine, oceanography or engineering. In economics, wavelet analysis was first considered in articles by, e.g., Ramsey et al. (1995), Ramsey and Lampart (1998) and Gençay et al. (2001), but its advantages, in contrast to other sciences, have not been extensively exploited yet. A review of different wavelet concepts with a focus on economic applications is given by Crowley (2007). Wavelet functions which are the building block of the wavelet approach are, unlike the sine and cosine functions used in spectral analysis, local in both the time and frequency domains, which makes wavelets suited to capture changes in behavior patterns. Wavelet analysis can therefore reveal how the relationship between different periodic components of time series evolves over time. This property enables us to obtain a more comprehensive picture of real wage cyclicality. Better understanding of the nature of cyclical behavior of real wages can be of great relevance for monetary policy.

This article is also an attempt to provide a reliable comparison of the real wage cyclicality in the USA and Germany. Given the differences in statistical classifications as well as the availability of the data in both countries, we consider the most comparable sectors of industry in the USA and Germany. To avoid possible influences of different seasonal adjustment methods, we use raw data.

Furthermore, we apply two different methods to estimate cycles from time series to check the robustness of the findings: the first one uses the structural time series (STS) model proposed by Harvey (1989) and the second one consists of the ARIMA–model–based (AMB) approach (see, e.g., Box et al., 1978) combined with the canonical decomposition (see Hillmer and Tiao, 1982) and the application of a band–pass filter based on a Butterworth tangent filter (see Gómez, 2001). A great advantage of these methods is that they are well suited to remove seasonality from the data. Moreover, they also take into account the stochastic properties of the data as opposed to ad hoc filtering methods like the filters proposed by Hodrick and Prescott (1997) or Baxter and King (1999), which are very popular in macroeconomic applications, mostly because of their convenient implementation. Since the results may also be affected by the price deflator used to compute real wages, we distinguish between consumer real wages and producer real wages.

The remainder of the article is organized as follows. In Section 2 we apply two decomposition methods to the industrial production index (IPI), consumer real wages and producer real wages in the USA and Germany. In Section 3.1 we set out the most important wavelet concepts. More detailed explanations of one of them, the wavelet phase angle, are provided in Section 3.2. In Section 3.3 it is shown how the previously introduced concepts are implemented in our study. In Section 3.4 we examine the comovements between the particular IPI cycle and the corresponding real wage cycles in the time–frequency domain using wavelet analysis. Section 4 summarizes the results and concludes.

2 Cyclical component

We assume that the time series under consideration or the log of it can be expressed as the sum of several unobserved components. Under this assumption, the series of interest is usually decomposed as

$$y_t = p_t + s_t + c_t + i_t, \tag{1}$$

where p_t is the trend, s_t is the seasonal, c_t is the cyclical and i_t is the irregular component. The different components are assumed to be uncorrelated and they are best defined in the frequency domain. Thus, the trend component is associated with a spectral peak at the zero frequency, the seasonal component has spectral peaks at the seasonal frequencies, defined as $2\pi k/s$, $k = 1, 2, \ldots, [s/2]$, where s is the number of seasons and $[s/2]$ denotes the integer part of $s/2$, and the irregular component is usually assumed to be white noise.[1] Finally, for economic series, the cyclical component is supposed to have some spectral peak in a frequency band corresponding to periods between 1.5 and 8 years. Since the relationship between frequency ω and period p is given by the formula $p = 2\pi/\omega$, the cyclical band for quarterly series is $[\pi/16, \pi/3]$.

To estimate the cyclical component, c_t in (1), the usual approach in economics is to apply a fixed filter, like the Hodrick–Prescott or the Baxter–King filter. However, this approach has its limitations because it does not take into account the stochastic characteristics of the series at hand. For example, it is well known that one can generate spurious cycles if one applies a fixed filter to a white noise series. For this reason, in this article we propose to use two model–based methods to estimate the cycle in an economic time series.

The first method is based on the so–called structural models introduced by Harvey (1989). These models assume a decomposition of the form (1), where the components follow certain ARIMA models. See Harvey (1989) for details. The model can be put into state space form and the Kalman filter and smoother can be used to estimate the unobserved components. It is to be noted that in this approach the models for the components are specified beforehand.

The second method consists of the AMB approach combined with the canonical decomposition and the application of a band–pass filter. It has two steps. In the first one, an ARIMA model is specified for the series and the canonical decomposition is used to derive models for the trend–cycle, seasonal and irregular components (see Hillmer and Tiao, 1982). In the second step, the cycle is estimated by the application of a band–pass filter, designed to extract the random elements in the cyclical frequency band, to the trend–cycle obtained in the first step. The procedure is fully model–based and is described in Gómez
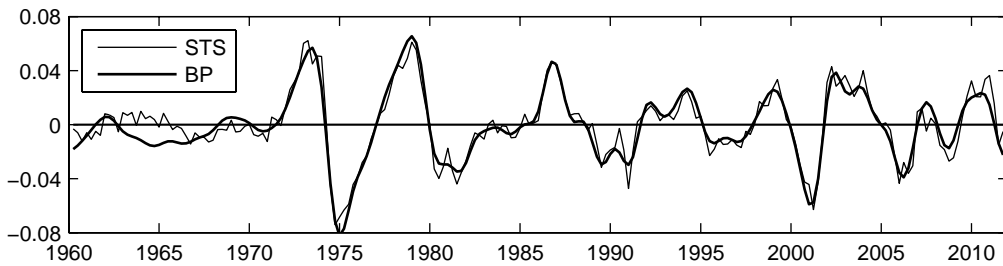
---

[1]For a nonstationary series we would consider the pseudospectrum instead of the spectrum.
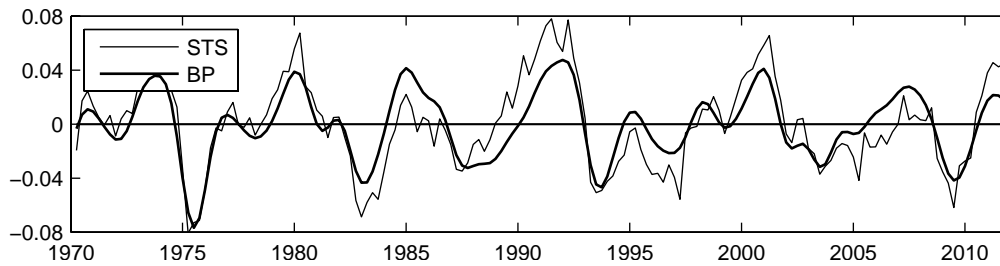
(a) Cycles of the industrial production index (IPI)
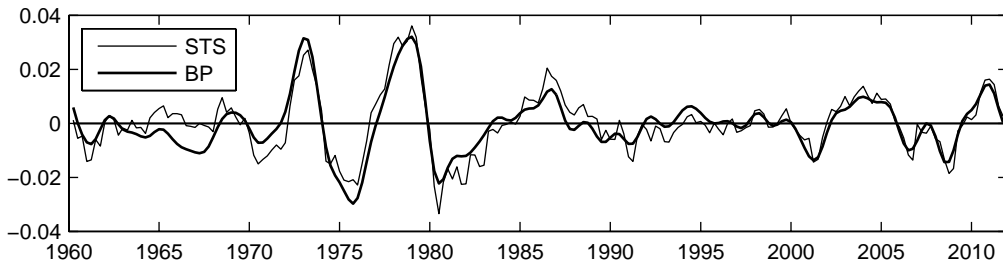
(b) Cycles of the consumer real wage

(c) Cycles of the producer real wage

Figure 1: US cycles of the IPI and real wages based on the STS approach and a band–pass (BP) filter

(2001). Once models for the different components, including the cycle, are obtained, the overall model can be put into state space form and the Kalman filter and smoother can be applied to estimate the components as in the first method.

Although both methods are model based, the second one is more likely to extract smoother, more definite, cycles because only those random elements corresponding to the cyclical frequency band are passed by the band–pass filter. The cycle estimated with structural models will usually be less smooth. In order to get smoother cycles with structural models, one should use the generalized cycle models of Harvey and Trimbur (2003). However, the cycles estimated with structural models will be satisfactory enough
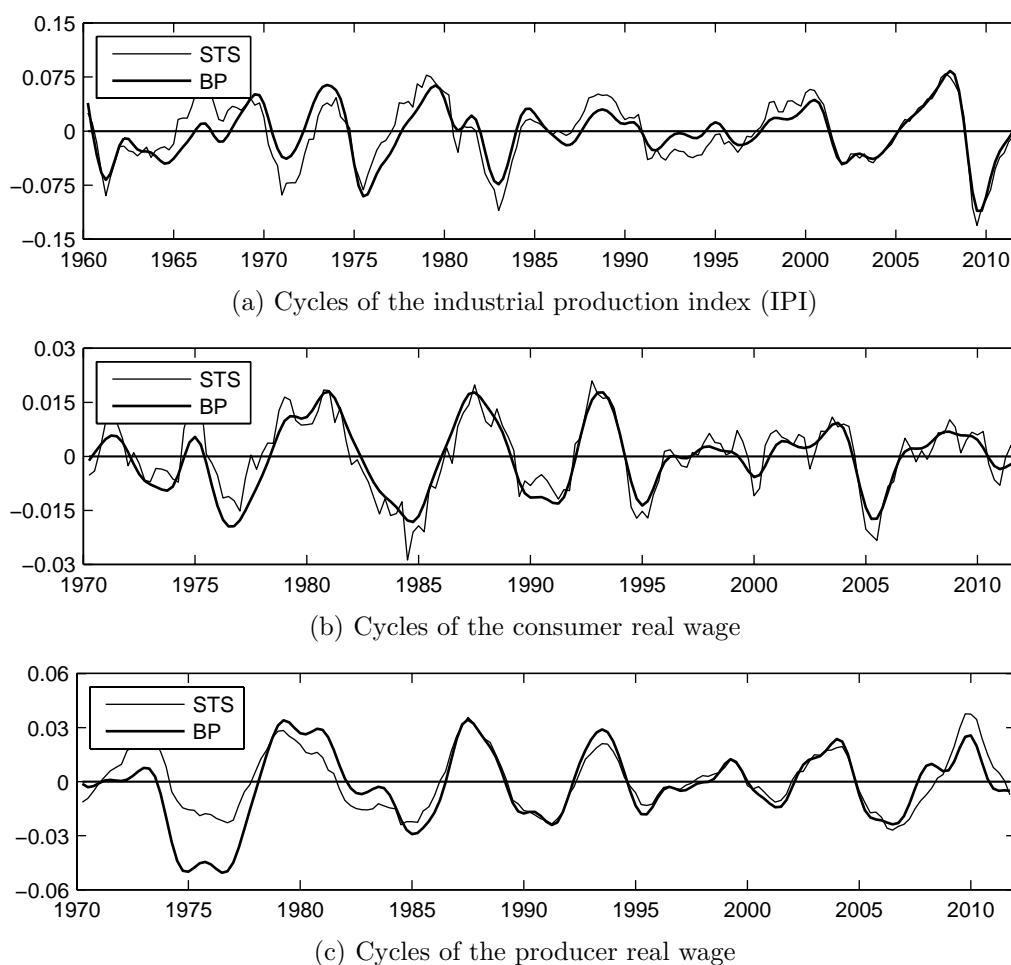
4

(a) Cycles of the industrial production index (IPI)

(b) Cycles of the consumer real wage

(c) Cycles of the producer real wage

Figure 2: German cycles of the IPI and real wages based on the STS approach and a band–pass (BP) filter

for the purposes of this article.[2]

In Figure 1, one can see the cycles estimated with both methods for the US series. As expected, the cycles estimated with the band–pass filter are smoother than the cycles estimated with the structural models.

The cycles estimated with both methods for the German series are displayed in Figure 2. Here, one can also see that the cycles estimated with the band–pass filter are smoother.

---

[2]We use the SSMMatlab toolbox to perform all necessary computations (see Gómez, 2012). Only the identification of an ARIMA model and outlier and regression effects for the series at hand for the AMB approach is made using program TRAMO (see Gómez and Maravall, 1996). The same outlier and regression effects are used with structural models.

3 Comovements of real wages and the business cycle: wavelet analysis

3.1 Wavelet concepts

In the economic literature on wavelet analysis, three directions emerged: the continuous wavelet transform (CWT) (see, e.g., Rua and Nunes, 2009), the discrete wavelet transform (see, e.g., Crowley and Mayes, 2008) and the maximum overlap discrete wavelet transform (see, e.g., Gallegati et al., 2011). They differ in the way how a function of time is mapped onto the time–frequency plane. Our analysis relies on the CWT. In this section, we resort to some key concepts associated with this type of transform.

The building block of wavelet analysis is the so–called mother (or analyzing) wavelet, denoted herafter as ψ. Suppose that ψ is a real– or complex–valued function in $L^1(\mathbb{R}) \cap L^2(\mathbb{R})$, i.e. :

$$\int_{-\infty}^{\infty} \psi(t)dt < \infty, \qquad \int_{-\infty}^{\infty} |\psi(t)|^2 dt < \infty \tag{2}$$

In other words, ψ has finite energy since it holds:

$$\|\psi\|^2 = \langle \psi, \psi^* \rangle = \int_{-\infty}^{\infty} |\psi(t)|^2 dt, \tag{3}$$

where $\| \cdot \|$ and $\langle \cdot \rangle$ denote the norm and the inner product, respectively, and ψ^* is the complex conjugate of ψ. Function ψ qualifies for the mother wavelet, if it satisfies the admissibility condition (see, e.g., Farge, 1992; Daubechies, 1992, p. 24):

$$0 < C_\psi = \int_{-\infty}^{\infty} \frac{|\Psi(\omega)|^2}{|\omega|} d\omega < \infty, \tag{4}$$

where ω is the angular frequency, $\Psi(\omega)$ is the Fourier transform of $\psi(t)$ and C_ψ is called the admissibility constant. The admissibility condition implies

$$\Psi(0) = \int_{-\infty}^{\infty} \psi(t)dt = 0$$

Along with the sufficient decay property, this ensures localization in both time and frequency. Moreover, it is usually assumed that $\|\psi\| = 1$, implying unit energy of ψ. On the basis of the mother wavelet, a doubly–indexed family of wavelets is generated by the so–called translation and dilation (scaling) of ψ:

$$\psi_{\tau,s}(t) = \frac{1}{\sqrt{|s|}} \psi\left(\frac{t-\tau}{s}\right), \qquad \tau, s \in \mathbb{R}, s \neq 0 \tag{5}$$

Translation leads to a shift of ψ by the so–called translation parameter τ. Dilation, on the other hand, reduces or increases the support of ψ, if $|s| < 1$ or $|s| > 1$, respectively, where s is the so–called dilation (scaling) parameter. The factor $1/\sqrt{|s|}$ guarantees that $\psi_{\tau,s}$ preserves unit energy.

The CWT of a continuous function x in $L^2(\mathbb{R})$ is given by:

$$
\begin{aligned}
W_{x,\psi}(\tau, s) &= \langle x(t), \psi_{\tau,s}^*(t) \rangle \\
&= \int_{-\infty}^{\infty} x(t) \frac{1}{\sqrt{|s|}} \psi^* \left(\frac{t - \tau}{s} \right) dt
\end{aligned}
\tag{6}
$$

Parseval's relation $\langle x, \psi \rangle = (1/2\pi) \langle X, \Psi \rangle$, where X is the Fourier transform of x, allows to write $W_{x,\psi}(\tau, s)$ as:

$$
W_{x,\psi}(\tau, s) = \frac{\sqrt{|s|}}{2\pi} \int_{-\infty}^{\infty} \Psi^*(s\omega) \, X(\omega) \, e^{i\omega\tau} d\omega
\tag{7}
$$

Note that in eq. (6) and (7) τ corresponds to the time dimension, whereas s refers to the scale dimension, implying that $W_{x,\psi}(\tau, s)$ provides a time–scale representation of the analyzed function x. A particular scale represents a frequency band which makes it difficult to interpret the frequency content of x directly (see, e.g., Sinha et al., 2005). However, it is possible to convert scales into Fourier (or angular) frequencies, as there exists a formula that makes use of the so–called center frequency of the wavelet and states an inverse relation between scale and frequency (see, e.g., Abry et al., 1995). For an appropriate choice of the functional form of the wavelet, this relation becomes more straightforward and facilitates the interpretation of the wavelet transform in terms of frequency. In such a case, we will use the terms scale and frequency interchangeably.

The wavelet power spectrum of x is obtained as:

$$
P_{x,\psi}(\tau, s) = |W_{x,\psi}(\tau, s)|^2
\tag{8}
$$

and represents the local variance of x. If the time–frequency relationship between two time series is of interest, it can be measured by the so–called wavelet cross–spectrum interpreted as the local covariance between these time series. For a pair of functions x and y, both in $L^1(\mathbb{R}) \cap L^2(\mathbb{R})$, the wavelet cross–spectrum is defined as (see Hudgins et al., 1993):

$$
W_{xy,\psi}(\tau, s) = W_{x,\psi}(\tau, s) \, W_{y,\psi}^*(\tau, s)
\tag{9}
$$

In general, eq. (9) can also be written as:

$$W_{xy,\psi}(\tau, s) = \Re(W_{xy,\psi}(\tau, s)) + \Im(W_{xy,\psi}(\tau, s)) \tag{10}$$

$$= |W_{xy,\psi}(\tau, s)| \; e^{\;\phi_{xy,\psi}(\tau, s)}, \tag{11}$$

where $\Re(W_{x,y;\psi}(\tau, s))$ denotes the wavelet co–spectrum and $\Im(W_{x,y;\psi}(\tau, s))$ is the wavelet quadrature spectrum, whereas $\phi_{xy,\psi}(\tau, s)$ in the polar form (11) corresponds to the wavelet phase angle. If $W_{xy,\psi}(\tau, s)$ is real, the quadrature spectrum and the phase angle are both zero. As the economic data are, in general, real–valued, it is evident that $W_{xy,\psi}$ can be complex–valued only for complex ψ. In the following, we consider only the case of complex wavelet functions since they allow for better insight into the comovement between two series by decoupling the amplitude and the phase angle.

In the literature, one can find several concepts that build on the information contained in the wavelet cross–spectrum. The most common ones are wavelet coherency and wavelet squared coherency, also called wavelet coherence (see, e.g., Liu, 1994). Both can be seen as the counterparts of the frequency–domain coherency and coherence, respectively. Wavelet coherency is given by:

$$R_{xy,\psi}(\tau, s) = \frac{W_{xy,\psi}(\tau, s)}{|W_{x,\psi}(\tau, s)| \; |W_{y,\psi}(\tau, s)|} \tag{12}$$

Since $W_{xy,\psi}(\tau, s)$ directly enters the formula for $R_{xy,\psi}(\tau, s)$, wavelet coherency is, like wavelet cross–spectrum, complex–valued and therefore difficult to interpret. For that reason, the concept of coherency will not be pursued in this study. Square of the wavelet coherency, wavelet coherence, is defined as:

$$R_{xy,\psi}^2(\tau, s) = \frac{|W_{xy,\psi}(\tau, s)|^2}{|W_{x,\psi}(\tau, s)|^2 \; |W_{y,\psi}(\tau, s)|^2} \tag{13}$$

$$= \frac{[\Re(W_{xy,\psi}(\tau, s))]^2 + [\Im(W_{xy,\psi}(\tau, s))]^2}{|W_{x,\psi}(\tau, s)|^2 \; |W_{y,\psi}(\tau, s)|^2} \tag{14}$$

Since the sample analog of $R_{xy,\psi}^2(\tau, s)$ takes on the value one for all τ and s, Liu (1994) suggests to analyze the real and the imaginary parts separately in order to avoid this problem. We follow the approach of Torrence and Webster (1999) and reformulate $R_{xy,\psi}^2(\tau, s)$ as

$$R_{xy,\psi}^2(\tau, s) = \frac{S(|W_{xy,\psi}(\tau, s)|^2)}{S(|W_{x,\psi}(\tau, s)|^2) \; S(|W_{y,\psi}(\tau, s)|^2)}, \tag{15}$$

where S denotes a smoothing operator in both time and scale. Smoothing is achieved by a convolution of the function to be smoothed and a window function. The wavelet coherence is one of the two comovement concepts used in this article. The other one, the wavelet phase angle, is explained in more detail in the next subsection.

3.2 Wavelet phase angle and its interpretation

Despite of its usefulness in measuring the strength of the time–frequency relationship, $R^2_{xy,\psi}(\tau, s)$ is able neither to determine the direction (positive or negative) of this relationship nor to establish the lead–lag relation between the series at hand. For this purpose, the concept of the phase angle is well suited. The wavelet phase angle that has been already introduced in eq. (11) is defined as:

$$\phi_{xy,\psi}(\tau, s) = \arctan \left[\frac{\Im(W_{xy,\psi}(\tau, s))}{\Re(W_{xy,\psi}(\tau, s))} \right] \tag{16}$$

From the properties of arctangent it follows that the phase angle $\phi_{xy,\psi}(\tau, s)$ is a multi-valued function. For given τ and s, the values of arctangent are given by the respective principal value $\pm n\pi$, where $n = 0, 1, 2...$ and the principal value lies in $(-\pi/2, \pi/2)$. It is common to limit values of the phase angle to the interval $[-\pi, \pi]$.[3] Note that $\phi_{xy,\psi}(\tau, s) \equiv \pm\pi/2$ for $\Re(W_{xy,\psi}(\tau, s)) = 0$ and $\Im(W_{xy,\psi}(\tau, s)) \gtrless 0$. If, for specific τ and s, the relation $0 < \phi_{xy,\psi}(\tau, s) < \pi$ occurs, y is said to lag x at (τ, s). The opposite case is implied by $-\pi < \phi_{xy,\psi}(\tau, s) < 0$. Both series are in phase for particular (τ, s), if $\phi_{xy,\psi}(\tau, s)$ equals zero. Based on the values of the phase angle we can also make statements about the in–phase or anti–phase relation between the components of x and y. If the values of the phase angle range between $(-\pi/2, \pi/2)$, the respective components are positively related to each other (procyclical behavior/in–phase movement), whereas the values of $\phi_{xy,\psi}(\tau, s)$ in the interval $[-\pi, -\pi/2)$ or $(\pi/2, \pi]$ indicate a negative relationship (countercyclical behavior/anti–phase movement) between them. The interpretation of the phase angle values is summarized in Figure 3.

Sometimes, if knowledge about the mean direction of the relationship between time series is desired, it can prove convenient to analyze the mean phase angle. Due to the

---

[3]Marczak and Beissinger (2012) provide a rationale for this common practice and an interpretation of the values of the phase angle.
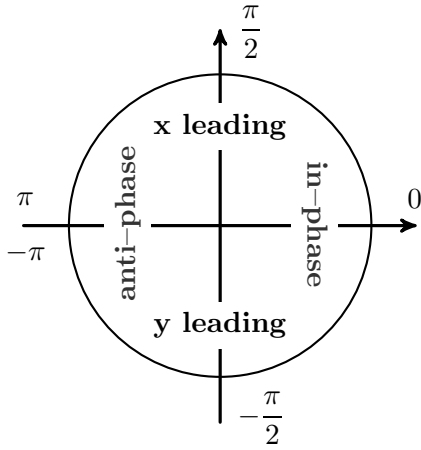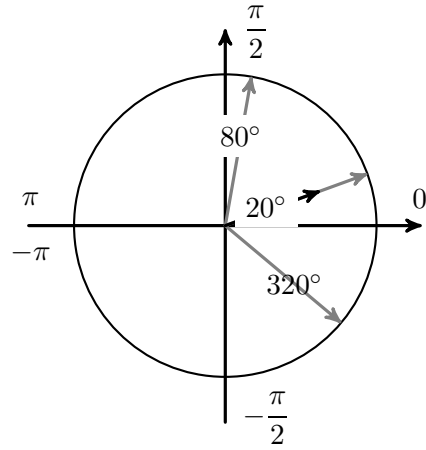
Figure 3: Interpretation of the phase angle

Figure 4: Example of a mean of the phase angle samples

circular nature of the phase angle, the standard arithmetic mean fails to be an appropriate technique for that purpose. Instead, the concept of a mean specially devoted to the data measured on the angular scale should be employed (see, e.g., Zar, 1999). This concept rests on the fact that for any phase angle ϕ_i it holds that $\tan(\phi_i) = \sin(\phi_i)/\cos(\phi_i)$. Thus, ϕ_i can be represented in the Argand diagram as the angle between the positive half of the real axis and the unit length vector $r_i = (\cos(\phi_i), \sin(\phi_i))$. Averaging over all $r_i, i = 1, ..., n$, where n is the length of the sample of the phase angles, leads to the so–called mean resultant vector $\bar{r}$. The mean phase angle $\bar{\bar{\phi}}$ is then obtained as $\arctan(\bar{r}_2/\bar{r}_1)$, where $j = 1, 2$ denotes the jth element in $\bar{r}$. In addition, the length of $\bar{r}$ ($\bar{r}$), ranging from zero to one, quantifies the concentration of the sample around $\bar{r}$ and, therefore, it plays an important role in significance testing. Values $\bar{r}$ closer to zero (one) indicate higher (smaller) circular spread within the sample. Figure 4 illustrates the idea of the mean for circular data with an example of three phase angle values: $20°, 80°$ and $320°$. It is evident that the arithmetic mean being equal to $140°$ would be a misleading measure of the mean since the vectors (gray) corresponding to the sample phase angles point all to the right. The mean resultant vector (black) of length 0.667 points to the same direction and implies the mean value $20°$.

3.3 Implementation of wavelet concepts and significance testing

In empirical applications involving wavelets, one of the choices to be made concern the selection of the functional form of the wavelet. As has been pointed out in section 3.1, in the case of real–valued series it is more informative to use complex wavelets. We consider the so–called Morlet wavelet which is a complex–valued continuous function:

$$\psi_{\omega_0}(t) = \pi^{-1/4} \left(e^{i\omega_0 t} - e^{-\omega_0^2/2} \right) e^{-t^2/2},$$

where $\pi^{-1/4}$ is a normalization factor. Expression $e^{\omega_0^2/2}$ represents the correction term to enforce the term in brackets to have zero mean, thereby ensuring that the admissibility condition is satisfied. One of the advantages of the Morlet wavelet is that the aforementioned inverse relation between scale s and Fourier frequency f (or angular frequency ω) becomes very simple for the common choice $\omega_0 = 6$, i.e. $f \approx 1/s$ ($\omega \approx 2\pi/s$).

Moreover, the Morlet wavelet allows for the optimal time–frequency localization. According to the Heisenberg uncertainty principle, there is always a trade–off between the precisions obtained in the time and frequency spaces. It can be shown that for the Morlet wavelet with $\omega_0 = 6$, total uncertainty is minimized, and, in addition, the uncertainty associated with time localization is equal to that associated with frequency localization so that the best time–frequency balance can be attained (see Aguiar-Conraria and Soares, 2011b).

As outlined before, we restrict ourselves to the usage of the wavelet coherence and the wavelet phase angle. Since we are dealing with discrete data, the wavelet measures described in section 3.1 have to be discretized. Derivation of the discrete version of the CWT in eq. (7) which can serve as a basis for the discrete version of the other wavelet tools is presented by Aguiar-Conraria and Soares (2011b). Due to the finite length of the series, it is common to pad the series with zeros prior to the application of the transform. This procedure helps to avoid wrap–around effects that arise because the used discrete Fourier transform assumes that the data are periodic. However, zero–padding also leads to underestimation of the CWT values near the ends of the sample. This problems becomes more severe with increasing scales as the wavelet support increases and hence more zeros are involved in the computation of the CWT at the beginning and at the end of the series. Regions affected from these border distortions are called cone of influence (COI). Values

of the wavelet measures that fall into the COI should be interpreted with caution.[4]

The calculated measures are estimates of their theoretical counterparts and therefore it is important to assess the significance of the results. One of the first works where the significance issue is addressed in the context of wavelet analysis is the article by Torrence and Compo (1998) who obtain the empirical distribution for the wavelet power spectrum as well as for the wavelet cross–spectrum. Even though computationally very efficient, this approach has some drawbacks, for example it is applicable only to these two measures and it requires specific assumptions for the derivation of the distribution. An alternative to this kind of significance test are tests that rely on bootstrapped data. Some authors apply nonparametric bootstrap methods, as, e.g., Cazelles et al. (2007). In contrast, in their examples with economic data Aguiar-Conraria and Soares (2011b) consider a parametric approach and generate new samples by bootstrapping ARMA models for the analyzed data, for instance the cycles. We build on the approach proposed by Stoffer and Wall (1991) whereby we exploit the state space representation with which the original cycle estimates were obtained. In this way, we avoid imposing models for the estimated cycles or making additional choices needed for nonparametric methods, as for example selection of the block size when resampling blocks of data (see Berkowitz and Kilian, 2000). More specifically, we proceed in two steps. In the first one, we obtain bootstrap samples of the observations. For that purpose, we first perform bootstrapping on the standardized innovations resulting from the estimation of the models described in Section 2 and then with the estimated matrices of the state space models and each bootstrap sample of standardized innovations we construct a set of observations. In the second step, using each of the bootstrap samples of observations we get a set of smoothed cyclical components using the Kalman smoother. In wavelet analysis, we resort to the bootstrapped cycles when computing the bootstrapped values of the wavelet coherence. For identification of the significant regions of coherence, we draw on p–values based on the replicated coherence

---

[4]Computation of $R^2_{xy,\psi}(\tau, s)$ and $\phi_{xy,\psi}(\tau, s)$ is carried out using programs based on the ASToolbox by Aguiar-Conraria and Soares (2011a). Mean values of $\phi_{xy,\psi}(\tau, s)$ are obtained with the CircStat Toolbox by Berens (2009). For graphical illustration of these measures, we utilize modified programs from the toolbox by Grinsted et al. (2008).

values.[5]

3.4   Results

The results for the US case are presented in Figures 5 and 6. Figure 5 shows the estimated wavelet coherence and phase angle for the IPI cycles acting as business cycle indicators and the consumer real wage cycles, whereas Figure 6 contains the corresponding estimation results for the IPI cycles and the producer real wage cycles. The left panel of the figures refers to the cycles obtained with the STS approach and the right panel corresponds to the band–pass cycles. For ease of reference, scales at which the wavelet measures have been computed are converted to periods according to the formula $p = 2\pi/\omega$, where p denotes the period and ω is the frequency which is in this case, as mentioned in the previous subsection, derived as $\omega = 2\pi/s$. It should be noticed that the considered periods cover all business cycle periodicities, i.e. periods between 1.5 and 8 years. Figures in the upper row depict the estimated time–frequency wavelet coherence and phase angle. Low values of the coherence are represented by regions not covered by arrows. In the remaining region, light areas designating medium values fade into dark areas corresponding to the strongest coherence. Areas delimited by the black lines cover coherence values that are significant at the 5% level. Values of the time–frequency phase angle are illustrated by arrows. Direction of an arrowhead can be related to the phase angle in the unit circle and can be thus interpreted as shown in Figure 3. Arrows pointing to the right/left indicate an in–phase/anti–phase relationship between the real wage cycle and the business cycle. Arrows pointing up/down suggest lagging/leading of the real wage cycle over the business cycle. Shaded regions outside the downward and upward sloping lines towards the beginning and the end of the sample, respectively, show the COI. The figures in the middle and in the lowest part illustrate the phase angle averaged over scales corresponding to the business cycle periodicities, and the phase angle averaged over time, respectively. Black lines give the 95% confidence bounds for the mean values depicted by dots.

In Figures 5a and 5d, it is apparent that, irrespective of the decomposition method,

---

[5]For the generation of the bootstrapped cycles, we use the procedures bootsam and bootcomp from the SSMMatlab toolbox. Confidence intervals for the mean values of $\phi_{xy,\psi}(\tau, s)$ are calculated with the CircStat Toolbox.

(a) Wavelet coherence and phase angle: STS

(d) Wavelet coherence and phase angle: BP

(b) Mean phase angle over scales: STS

(e) Mean phase angle over scales: BP

(c) Mean phase angle over time: STS
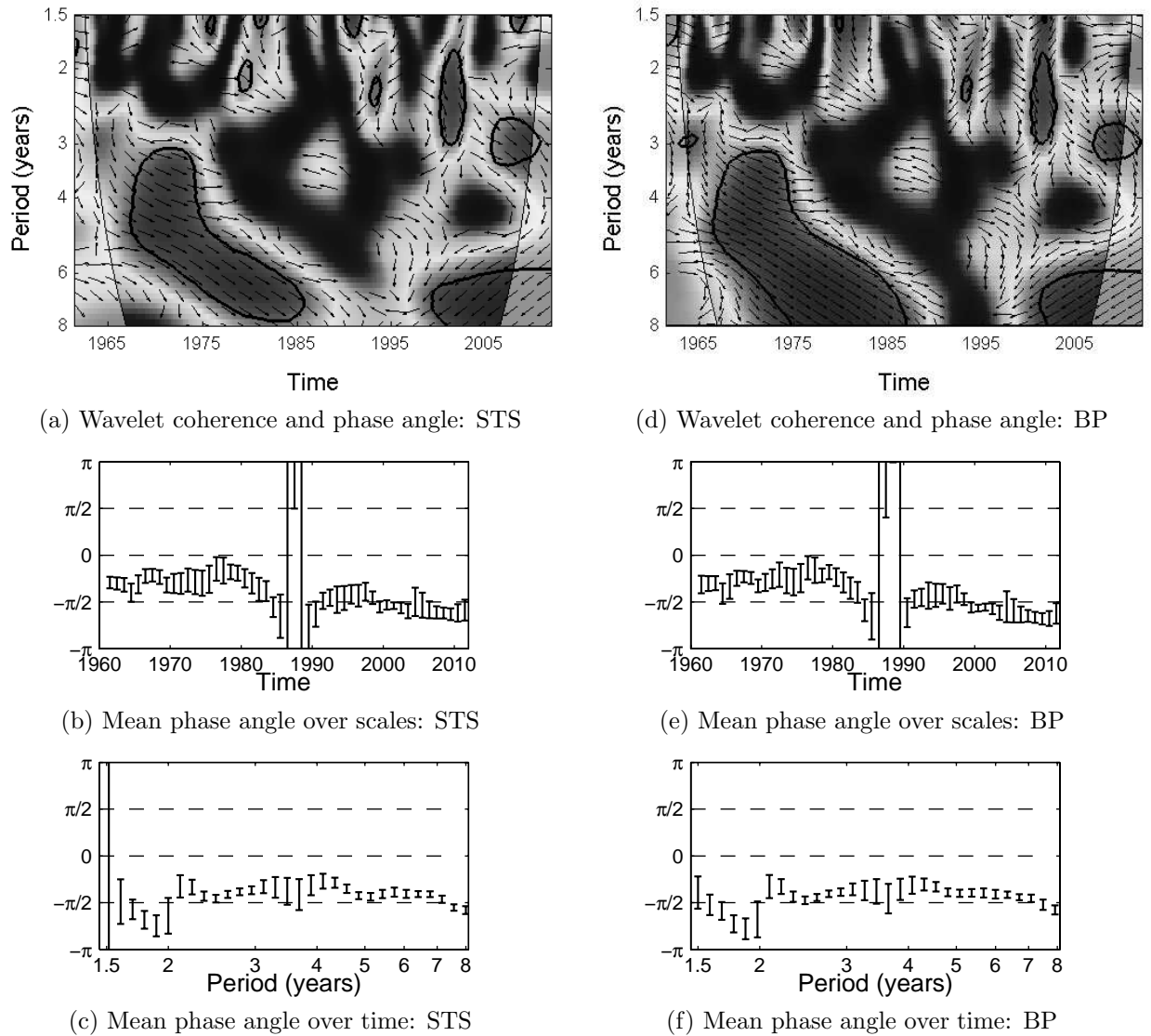
(f) Mean phase angle over time: BP

Figure 5: Wavelet coherence and phase angle: US IPI and US consumer real wage cycles based on the STS approach and a band–pass (BP) filter

Notes: a), d) Coherence ranges from low values (dark areas not covered by arrows) to high values (dark areas covered by arrows). Shaded regions outside the downward and upward sloping lines represent the COI. Black contours show significance at the 5% level based on p–values calculated with 1000 bootstrapped cycles. Arrows designate the phase angle (pointing right/left: in–phase/anti–phase, pointing up/down: lag/lead of the consumer real wage cycle). b), c), e), f) Points depict the mean values. Black lines correspond to their 95% confidence intervals.

the strongest and statistically significant coherence between the consumer real wage cycle and the IPI cycle can be observed between 1965 and 1985 and from about 2000 on. Arrows

pointing to the right between 1965 and 1985 reveal a procyclical pattern of the consumer real wage in this time interval. The greatest contribution to this behavior comes from the components with periodicities between approximately 3 and 8 years. In addition, the relevance of shorter period components decreases over time. After 2000, the consumer real wage becomes countercyclical at rather higher periods. The strongest coherence occurs at periodicities between 6 and 8 years. In contrast, lower periods are associated with a rather procyclical pattern. In the entire time interval, at least for significant coherence values, the consumer real wage is leading the business cycle. These observations can be confirmed by the mean phase averaged over scales (see Figures 5b and 5e). It takes negative values in the entire time span with an exception of single outlying positive values. However, we do not interpret these outliers as well as other mean values falling into the interval from 1985 to 1995 as they are not informative due to very low insignificant coherence in this time span. From 1965 to 1985 the mean phase angle values lie between 0 and $-\pi/2$, thereby indicating a clear–cut procyclical pattern. Towards the end of the sample, the mean values fall slightly below $-\pi/2$ which is the consequence of an important contribution of countercyclical low–frequency components of the IPI cycle and the consumer real wage cycle. It is also worth noting that, as is evident from Figures 5c and 5f, the components with periodicities above 2 years are on average in–phase, whereas the shorter components of the IPI cycle and the real wage cycle exhibit on average an anti–phase relation.

As regards the producer real wage, we find similar time–frequency behavior to the case of the consumer real wage (see Figures 6a and 6d). The only difference is that for the producer real wage we can detect more pronounced significant coherence between 1985 and 2000. It can be observed at lower periodicities, between about 3.5 to 4.5 years starting from 1985 and between 1.5 and 3 years until 2000. Change in the direction of arrows in the mid–1980's at almost all periods suggests a change from an in–phase into an anti–phase relation. Figures 6b and 6e show this trend explicitly. Taking all periods into account, the producer real wage becomes countercyclical in the early 1980's. In Figures 6c and 6f, it is evident that the components with periodicities up to approximately 4 years are responsible for the anti–phase behavior whereas the components between 4 and 7 years induce on average a procyclical behavior of the producer real wage. Across all periods and times, the producer real wage leads the business cycle.
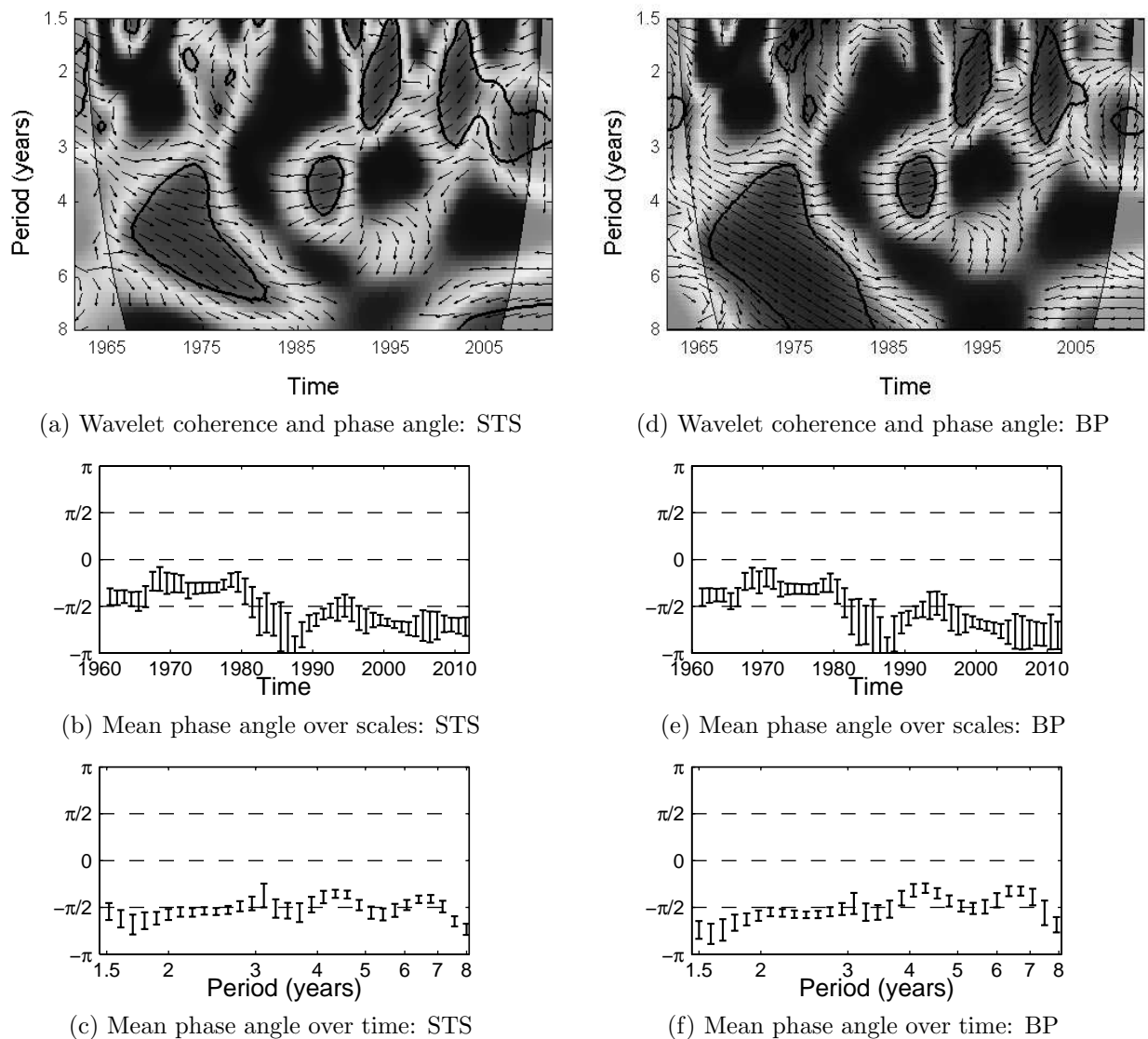
15

(a) Wavelet coherence and phase angle: STS

(d) Wavelet coherence and phase angle: BP

(b) Mean phase angle over scales: STS

(e) Mean phase angle over scales: BP

(c) Mean phase angle over time: STS

(f) Mean phase angle over time: BP

Figure 6: Wavelet coherence and phase angle: US IPI and US producer real wage cycles based on the STS approach and a band–pass (BP) filter

Notes: a), d) Coherence ranges from low values (dark areas not covered by arrows) to high values (dark areas covered by arrows). Shaded regions outside the downward and upward sloping lines represent the COI. Black contours show significance at the 5% level based on p–values calculated with 1000 bootstrapped cycles. Arrows designate the phase angle (pointing right/left: in–phase/anti–phase, pointing up/down: lag/lead of the consumer real wage cycle). b), c), e), f) Points depict the mean values. Black lines correspond to their 95% confidence intervals.

Summing up, both US real wages seem to have a similar scheme of comovements with the business cycle. They are leading the business cycle in the entire time interval and at all

periodicities. Until the mid–1980's, a procyclical pattern predominates. The significant coherence comes from the components in the range of middle and higher business cycle periodicities. Thereafter, the real wages become less procyclical and towards the end of the series even anticyclical.

The findings for Germany are summarized in Figures 7 and 8. As for the consumer real wage, Figures 7a and 7d show that the strongest coherence occurs until 1980 at periods up to about 4 years. From the mid–1980's to the mid–1990's, components with higher periodicities up to about 7 years are associated with strong, statistically significant coherence. Afterwards, the importance of lower components with lower and middle periodicities decreases. In contrast, the ones from the upper range of the business cycle periodicities make the major contribution to the overall coherence in this time interval. Arrows pointing up at all times and almost all periodicities indicate a lagging behavior of the consumer real wage in Germany. Significant values of the mean phase above $\pi/2$ illustrated in Figures 7b and 7e can be an evidence for a countercyclical consumer real wage in the considered time span. This anti–phase behavior is especially attributed to the components with periodicities below 6 years. At higher periodicities, we can identify a less anticyclical and even a slightly procyclical pattern.

After an inspection of Figures 8a and 8d, it becomes clear that despite of the similar significance regions for the wavelet coherence as in the case of the consumer real wage, the results for the producer real wage with respect to the lead–lag classification are not as homogeneous. Until the mid–1980' and from 2000 on, the producer real wage leads the business cycle whereas in the interval between 1985 and 2000, a lagging behavior of the producer real wage emerges (see Figures 8b and 8e). On average, the leading scheme can be assigned to the components up to approximately 4 years. In contrast, components with higher periodicities are responsible for the lagging scheme (see Figures 8c and 8f). In addition, we can detect an anti–phase relationship between the producer real wage and the business cycle across almost all times and periodicities, except for time periods prior to 1975. Analogous to the case of the consumer real wage, the negative relationship between the producer real wage cycle and the business cycle vanishes for periods above 6 years.
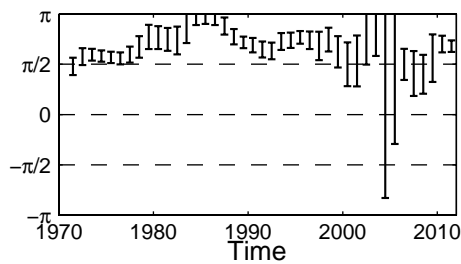
To sum up, German real wages turn out to be countercyclical in almost the entire
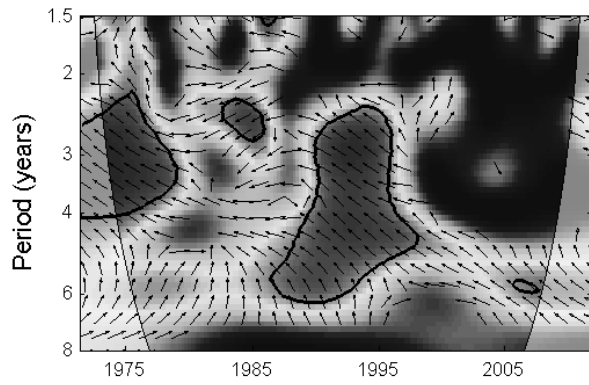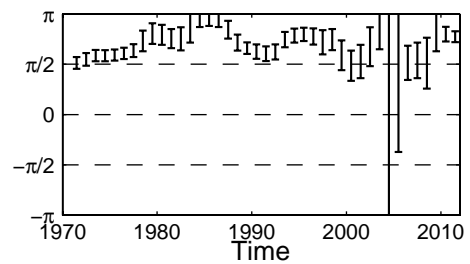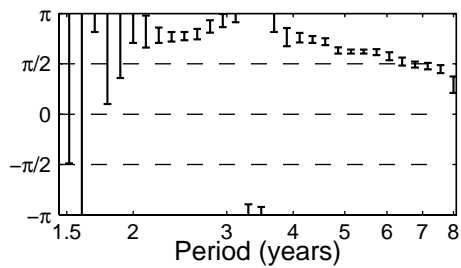
(a) Wavelet coherence and phase angle: STS
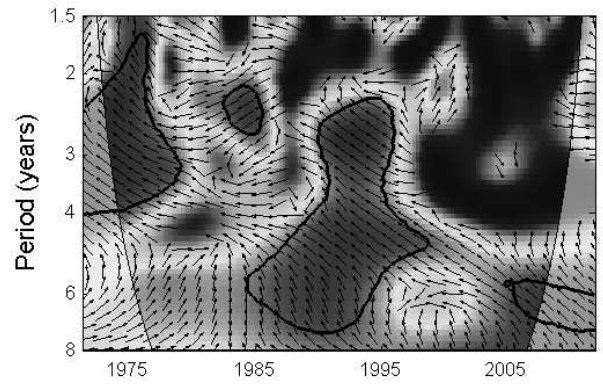
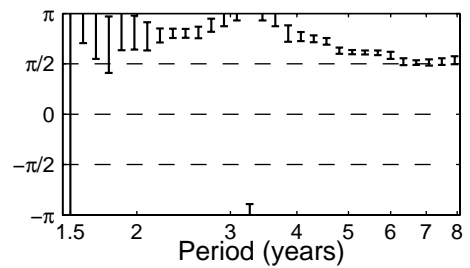(d) Wavelet coherence and phase angle: BP

(b) Mean phase angle over scales: STS

(e) Mean phase angle over scales: BP

(c) Mean phase angle over time: STS

(f) Mean phase angle over time: BP

Figure 7: Wavelet coherence and phase angle: German IPI and German consumer real wage cycles based on the STS approach and a band–pass (BP) filter

Notes: a), d) Coherence ranges from low values (dark areas not covered by arrows) to high values (dark areas covered by arrows). Shaded regions outside the downward and upward sloping lines represent the COI. Black contours show significance at the 5% level based on p–values calculated with 1000 bootstrapped cycles. Arrows designate the phase angle (pointing right/left: in–phase/anti–phase, pointing up/down: lag/lead of the consumer real wage cycle). b), c), e), f) Points depict the mean values. Black lines correspond to their 95% confidence intervals.

(a) Wavelet coherence and phase angle: STS

(d) Wavelet coherence and phase angle: BP

(b) Mean phase angle over scales: STS

(e) Mean phase angle over scales: BP

(c) Mean phase angle over time: STS

(f) Mean phase angle over time: BP

Figure 8: Wavelet coherence and phase angle: German IPI and German producer real wage cycles based on the STS approach and a band–pass (BP) filter

Notes: a), d) Coherence ranges from low values (dark areas not covered by arrows) to high values (dark areas covered by arrows). Shaded regions outside the downward and upward sloping lines represent the COI. Black contours show significance at the 5% level based on p–values calculated with 1000 bootstrapped cycles. Arrows designate the phase angle (pointing right/left: in–phase/anti–phase, pointing up/down: lag/lead of the consumer real wage cycle). b), c), e), f) Points depict the mean values. Black lines correspond to their 95% confidence intervals.
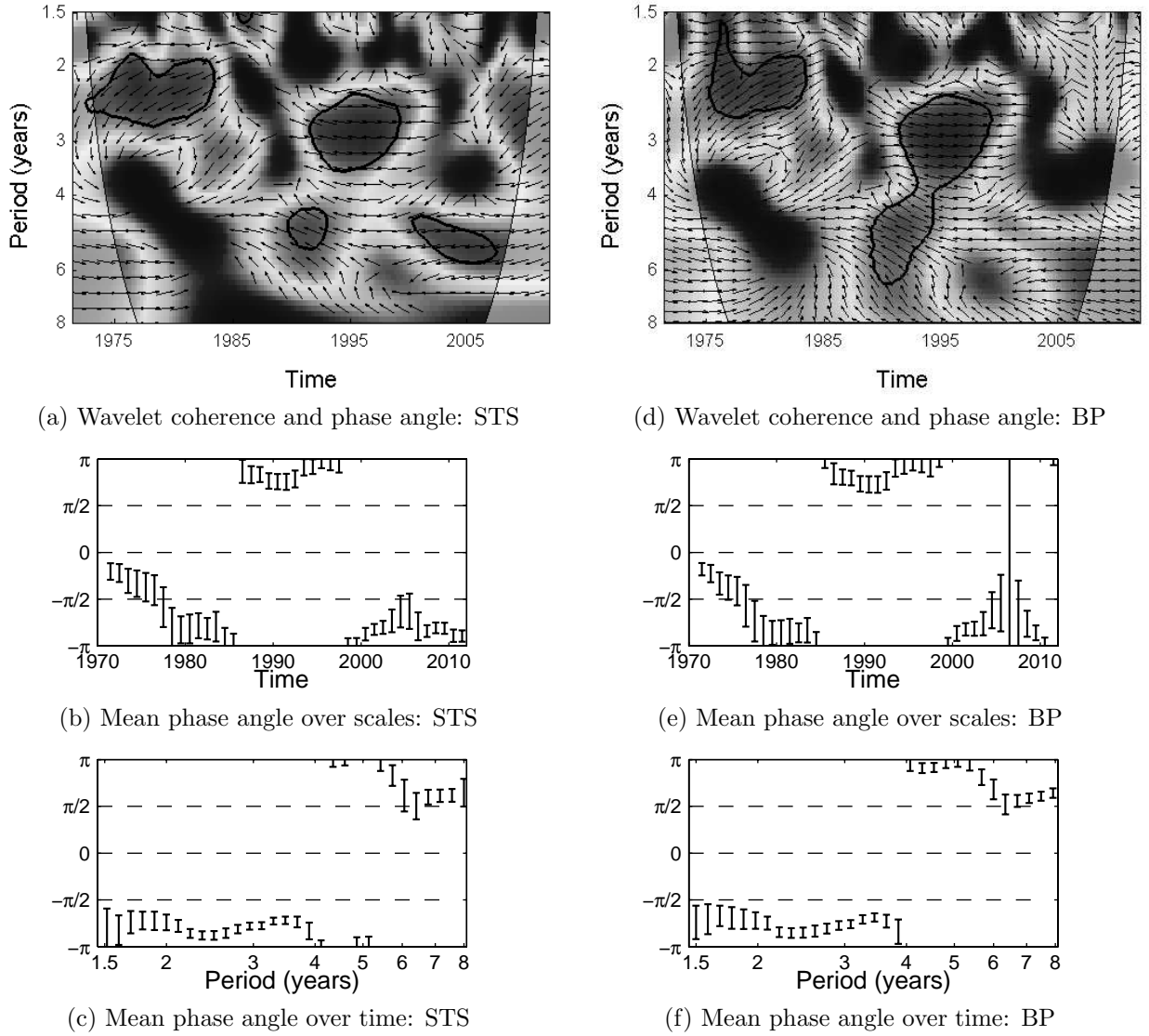
time span. As regards their behavior across different periodicities, the anti–phase relation is not present any more for higher periodicities. German consumer real wage is lagging

the business cycle at all times, as opposed to the producer real wage which is leading the business cycle from the mid–1980's to 2000. Similarly to the US case, the results remain robust independent of the decomposition method. All these observations resemble the findings in Marczak and Beissinger (2012) who apply the concept of the phase angle in the frequency domain to investigate the cyclical behavior of real wages in Germany in the whole economy.

A comparison of the results for the USA and Germany unveils the differences in the lead–lag behavior of real wages in both countries. Real wages in the USA are both leading the business cycle whereas in Germany the lead–lag relation with the business cycle differs between these real wage series. The consumer real wage in Germany reacts with delay to the actual economic situation. In contrast, the producer real wage is, at least for the most part of the considered time interval, leading the business cycle. Both countries also differ with respect to the regions with the strongest and statistically significant coherence. In the USA, they are observed from the mid–1960's to the mid–1980's and after 2000, whereas in the German case the most pronounced comovements are associated with time periods until the late 1970's and between about 1990 and 2000. Moreover, the classification of real wages as being in–phase or in anti–phase with the business cycle is differently distributed across periods in both countries. Apart from this discrepancy, we detect a similar overall tendency present in both countries – from a procyclical or an acyclical behavior prior to 1980 to an unambiguously countercyclical behavior thereafter.

Our results suggest that changes occurring over time could serve, along with differences in the used price deflators, in methods for measurement of comovements etc., as an additional possible explanation for differences in the comovement patterns detected in studies on real wage cyclicality. See Abraham and Haltiwanger (1995) for the discussion of different outcomes of analyses based on the US data. As for Germany, most of the few existing studies find that real wages are procyclical (see, e.g., Brandner and Neusser, 1992; Anger, 2007) or acyclical (see Pérez, 2001) which, generally speaking, contradicts the evidence from our analysis. However, it is worth noting that in these works the examined time intervals are usually shifted to the past by several years relative to the time interval considered in this article. Since, as shown before, the real wages seemed to exhibit a rather acyclical or procyclical behavior in the more distant past, this fact could explain

the contrasting outcomes of this article and most of the studies dealing with the German data.

4   Summary and Conclusions

This article sheds new light on the cyclical behavior of the consumer and producer real wages in the USA and Germany. As a tool to investigate comovements, we propose to use wavelet analysis enabling us to gain insights that cannot be provided by standard time–domain or spectral techniques. Wavelet methods can reveal whether the comovement pattern between components with particular periodicities is subject to any changes or whether it remains stable in the course of time. More specifically, we apply the concepts of wavelet coherence and wavelet phase angle. In order to establish the general tendency of the in–phase or anti–phase relation and the lead–lag relation between real wages and the business cycle across time periods and across different time horizons, we additionally interpret the mean phase angle over time and over business cycle periodicities, respectively. To obtain a robust and reliable picture on cyclicality of real wages, we apply two model–based methods for extraction of the cyclical components of the underlying time series: the structural time series (STS) approach and the ARIMA–model–based (AMB) approach combined with the canonical decomposition and a band–pass filter.

The analysis of the wavelet coherence and phase angle shows that the cyclicality in both countries is of a somewhat different nature. In the USA, the strongest and statistically significant coherence falls within the time interval from the mid–1960's to the mid–1980's and after 2000. On the contrary, the strongest and statistically significant coherence in Germany mainly pertains to the years until the late 1970's and the time period between 1990 and 2000. Furthermore, both US real wages are leading the business cycle in the entire time span and at most business cycle periodicities. In Germany, on the other hand, the outcomes depend on whether the consumer or the producer real wage is examined. For the consumer real wage, we find a lagging behavior at all times as well as at all business cycle periodicities. The producer real wage lags the business cycle only between 1985 and 2000 and only at the periodicities up to 4 years. Similarities between both countries emerge if we focus on the identification of the in–phase or anti–phase movements of real wages with the business cycle. Until 1980, real wages behave acyclically or procyclically

21

and they change their behavior to an anticyclical one afterwards. The detected cyclicality patterns for both real wages and both countries remain robust regardless of the methods used for the extraction of the cycles.

Appendix

A   Data Selection

In our analysis, we use raw quarterly data between 1960.Q1 and 2011.Q3 for the USA and between 1970.Q1 and 2011.Q3 for Germany. The US production index refers to the manufacturing sector after the SIC classification (source: Board of Governors of the Federal Reserve System, series: G.17). We obtained the US real wage series by deflating nominal hourly wages of production and nonsupervisory employees in manufacturing sector (source: FRED Economic Data, series ID: AHEMAN) with the consumer price index (source: FRED Economic Data, series ID: CPIAUCNS) or the producer price index (source: FRED Economic Data, series ID: PPIIDC). As for Germany, we use the production index in industry without construction that has already been linked over the annual average in 1991 (source: Deutsche Bundesbank, series ID: BBDE1.M.DE.N.BAA1.A2P200000.G.C.I05.L). Since, in contrast to the US case, nominal hourly wage series is not directly available, we create it by dividing the data on gross wages and salaries by the data on working hours, both corresponding to industry without construction. Prior to this, we link in both cases data sets up to 1991.Q4 referring to West Germany and from 1991.Q1 on referring to unified Germany over the annual averages in 1991. The source for the West German series is Statistisches Bundesamt, Fachserie 18, Reihe S.27 (revised quarterly results), whereas the source for the German series is Statistisches Bundesamt, GENESIS-Onlinedatenbank. The nominal hourly wages are in the next step deflated with the consumer price index (source: Deutsche Bundesbank, series ID: UUFB99) or the producer price index (source: Deutsche Bundesbank, series ID: UUZH99).

References

Abraham, K. G., and Haltiwanger, J. C. (1995). Real Wages and the Business Cycle. *Journal of Economic Literature*, *33*(3), 1215–1264.

Abry, P., Gonçalvès, P., and Flandrin, P. (1995). Wavelets, Spetrum Analysis and $1/f$ Processes. In A. Antoniadis and G. Oppenheim (Eds.), *Lecture Notes in Statistics* (Vol. 103, pp. 15–30). Springer.

Aguiar-Conraria, L., and Soares, M. J. (2011a). *ASToolbox.* Downloadable at `http://sites.google.com/site/aguiarconraria/joanasoares-wavelets/the-astoolbox`

Aguiar-Conraria, L., and Soares, M. J. (2011b). *The Continuous Wavelet Transform: A Primer* (NIPE Working Paper No. 16). Universidade do Minho.

Anger, S. (2007). *The Cyclicality of Effective Wages within Employer-Employee Matches: Evidence from German Panel Data* (Working Paper No. 783). ECB.

Baxter, M., and King, R. G. (1999). Measuring Business Cycles. Approximate Band-pass Filters for Economic Time Series. *Review of Economics and Statistics*, *81*(4), 575–593.

Berens, P. (2009). CircStat: A MATLAB Toolbox for Circular Statistics. *Journal of Statistical Software*, *31*(10), 1–21.

Berkowitz, J., and Kilian, L. (2000). Recent Developments in Bootstraping Time Series. *Econometric Reviews*, *19*(1), 1–48.

Box, G. E. P., Hillmer, S. C., and Tiao, G. C. (1978). Analysis and Modeling of Seasonal Time Series. In A. Zellner (Ed.), *Seasonal Analysis of Economic Time Series* (pp. 309–334). Washington, DC: U.S. Dept. Commerce, Bureau of the Census.

Brandner, P., and Neusser, K. (1992). Business Cycles in Open Economies: Stylized Facts for Austria and Germany. *Review of World Economics*, *128*(1), 67–87.

Brandolini, A. (1995). In Search of a Stylized Fact: Do Real Wages Exhibit a Consistent Pattern of Cyclical Variability? *Journal of Economic Surveys*, *9*(2), 103–163.

Cazelles, B., Chavez, M., de Magny, G. C., Guégan, J.-F., and Hales, S. (2007). Time–Dependent Spectral Analysis of Epidemiological Time–Series with Wavelets. *Journal of the Royal Society Interface*, *4*, 625–636.

Crowley, P. M. (2007). A Guide to Wavelets for Economists. *Journal of Economic*

Surveys, *21*(2), 207–267.

Crowley, P. M., and Mayes, D. G. (2008). An Evaluation of Growth Cycle Co-movement and Synchronization Using Wavelet Analysis. *Journal of Business Cycle Measurement and Analysis*, *4*(1), 63–95.

Daubechies, I. (1992). Ten Lectures on Wavelets. In *CBMS–NSF Conference Series in Applied Mathematics* (Vol. 61). Philadelphia: SIAM.

Farge, M. (1992). Wavelet Transforms and their Applications to Turbulence. *Annual Review of Fluid Mechanics*, *24*, 395–457.

Gallegati, M., Gallegati, M., Ramsey, J. B., and Semmler, W. (2011). The US Wage Phillips Curve across Frequencies and over Time. *Oxford Bulletin of Economics and Statistics*, *73*(4), 489–508.

Gençay, R., Selçuk, F., and Whithcher, B. (2001). Scaling Properties of Foreign Exchange Volatility. *Physica A: Statistical Mechanics and its Applications*, *289*, 249–266.

Gómez, V. (2001). The Use of Butterworth Filters for Trend and Cycle Estimation in Economic Time Series. *Journal of Business and Economic Statistics*, *19*(3), 365–373.

Gómez, V. (2012). *SSMMATLAB, a Set of MATLAB Programs for the Statistical Analysis of State–Space Models.* Downloadable at `http://www.sepg.pap.minhap.gob.es/sitios/sgpg/en-GB/Presupuestos/Documentacion/Paginas/SSMMATLAB.aspx`

Gómez, V., and Maravall, A. (1996). *Programs TRAMO and SEATS; Instructions for the User* (Working Paper No. 9628). Servicio de Estudios, Banco de España.

Grinsted, A., Moore, J. C., and Jevrejeva, S. (2008). *Cross Wavelet and Wavelet Coherence Package WTC-R16.* Downloadable at `http://www.pol.ac.uk/home/research/waveletcoherence/download.html`

Hart, R. A., Malley, J. R., and Woitek, U. (2009). Real Earnings and Business Cycles: New Evidence. *Empirical Economics*, *37*, 51–71.

Harvey, A. C. (1989). *Forecasting, Structural Time Series Models and the Kalman Filter.* Cambridge: Cambridge University Press.

Harvey, A. C., and Trimbur, T. M. (2003). General Model-Based Filters for Extracting Cycles and Trends in Economic Time Series. *Review of Economics and Statistics*, *85*(2), 244–255.

Hillmer, S. C., and Tiao, G. C. (1982). An ARIMA–Model–Based Approach to Seasonal Adjustment. *Journal of the American Statistical Association*, *77*(377), 63–70.

Hodrick, R. J., and Prescott, E. C. (1997). Postwar U.S. Business Cycles: An Empirical Investigation. *Journal of Money, Credit and Banking*, *29*, 1–16.

Hudgins, L., Friehe, C. A., and Mayer, M. E. (1993). Wavelet Transforms and Atmospheric Turbulence. *Physical Review Letters*, *71*(20), 3279–3282.

Liu, P. C. (1994). Wavelet Spectrum Analysis and Ocean Wind Waves. In E. Foufoula-Georgiou and P. Kumar (Eds.), *Wavelets in Geophysics* (pp. 151–166). London: Academic Press.

Marczak, M., and Beissinger, T. (2012). Real Wages and the Business Cycle in Germany. *Empirical Economics*, *DOI: 10.1007/s00181-011-0542-4*.

Messina, J., Strozzi, C., and Turunen, J. (2009). Real Wages over the Business Cycle: OECD Evidence from the Time and Frequency Domains. *Journal of Economic Dynamics and Control*, *33*(6), 1183–1200.

Pérez, P. J. (2001). *Cyclical Properties in the Main Western Economies* (Working Paper No. 33). The University of Manchester.

Ramsey, J. B., and Lampart, C. (1998). Decomposition of Economic Relationships by Time Scale Using Wavelets: Money and Income. *Macroeconomic Dynamics*, *2*, 49–71.

Ramsey, J. B., Usikov, D., and Zaslavsky, G. M. (1995). An Analysis of US Stock Price Behavior Using Wavelets. *Fractals*, *3*(2), 377–389.

Rua, A., and Nunes, L. (2009). International Comovement of Stock Market Returns: A Wavelet Analysis. *Journal of Empirical Finance*, *16*, 632–639.

Sinha, S., Routh, P. S., Anno, P. D., and Castagna, J. P. (2005). Spectral Decomposition of Seismic Data with Continuous–Wavelet Transform. *Geophysics*, *70*(6), 19–25.

Stoffer, D. S., and Wall, K. D. (1991). Bootstrapping State–Space Models: Gaussian Maximum Likelihood Estimation and the Kalman Filter. *Journal of the American Statistical Association*, *86*(416), 1024–1033.

Torrence, C., and Compo, G. P. (1998). A Practical Guide to Wavelet Analysis. *Bulletin of the American Meteorological Society*, *79*, 61–78.

Torrence, C., and Webster, P. J. (1999). Interdecadal Changes in the ENSO–Monsoon

System. *Journal of Climate*, *12*, 2679–2690.

Zar, J. H. (1999). *Biostatistical Analysis* (4th ed.). New Jersey: Prentice Hall.